Desalination and Water Treatment
www.deswater.com

19 (2010) 212–218
July

doi: 10.5004/dwt.2010.1887

Application of the SEBAL method in water resources management in the Yellow River Delta of China

Xiaoyan Wang[a,*], Chuangchun Zhang[b], Jiahua Wei[c]

[a]*College of Resources, Environment and Tourism, Capital Normal University, Beijing 100048, China*
email: wangxy@pku.edu.cn, cnuwxy@sohu.com
[b]*Research Center of International River, Ministry of Water resources of P.R .China, Beijing, China*
[c]*Department of Hydraulic and Hydropower Engineering, Tsinghua University, Beijing, China*

Received 18 September 2009; Accepted 22 February 2010

ABSTRACT

Evapotranspiration (ET) from agricultural fields, a consumptive use of fresh water for irrigation, is an important factor in water resources management in the Yellow River Delta (YRD) of China. Because the Surface Energy Balance Algorithm for Land (SEBAL) methodology requires a less ground measurements and includes the complete energy balance calculation, the algorithm was used to estimate ET as a component of the energy balance on a pixel-by-pixel basis in the YRD. Advanced Very High Resolution Radiometer and eight Landsat images covering the YRD were used to estimate both daily and monthly actual ET (ET_a) with the SEBAL method. The net crop water requirements (WRn) for the irrigated land were also estimated by subtracting the effective precipitation from the potential evapotranspiration (ET_p). The volume of net crop water requirements was obtained for the YRD area jointly with the digital crop maps and WRn values. Assessment of the performance of irrigated crops revealed that water delivery did not exceed the crop requirements, and the WRn for cotton and wheat were smaller than the irrigation demand. The result confirmed that the SEBAL model can estimate the ET_a and ET_p with higher accuracy, which will be an important tool in integrated water resources management and can provide spatial information to help decision-makers improve the current water use policies in the YRD.

Keywords: SEBAL; Water resources management; Evapotranspiration; Net crop water requirement; Yellow River Delta; Consumptive Use

1. Introduction

In recent years, water resources management has become very important. Especially, with the increased competition for fresh water between different users, monitoring the consumptive use of water by applying recently developed remote-sensing techniques has become one of the important issues in water resources management in the world. In the future, less water will be available for agricultural production due to competition with the industrial and domestic sectors, while at the same time food production must be increased to feed the growing population. Now water is becoming the limiting factor for agricultural production [1]. Evapotranspiration (*ET*) is the second most important component of the hydrologic cycle, behind precipitation. Therefore, estimation of the actual ET is very important for water resources management.

The application of the energy-balance equation to satellite remote sensing data has substantially matured over the past decades. Among several ET estimation methods, the remote sensing technology is regarded as the only technology that can efficiently and economically provide regional and global coverage of actual

*Corresponding author.

consumption [2]. Among the current satellite remote sensing models, the Surface Energy Balance Algorithm for Land (SEBAL) proposed and developed by Bastiaanssen [3–6] and the Surface Energy Balance System (SEBS) proposed by Su [7] had been designed to calculate the energy partitioning at the regional scale with minimal ground data and had been verified in many places in the world including China, Egypt, Sri Lanka, and other countries. SEBAL and SEBS were frequently applied in developing and developed countries, since they require a minimal amount of ground measurements including meteorological information. In addition, the confidence in the ET estimation is expected to increase with additional meteorological and ground information, when available. There were comprehensive reviews on remote sensing applications for agricultural water management [4, 8–10].

Irrigation performance assessment has been developed in the last 30 years. Bastiaanssen and Bos (1999) [11] reviewed the literature on irrigation performance indicators based on remotely sensed data, and gave some recommendations on how to more quickly take advantage of remote sensing capabilities to meet the present and near future challenges of agricultural water resources management. Bandara (2003) [12] described a framework for use of NOAA satellite data to assess operational irrigation performance, and applied the framework to irrigation schemes in the dry-zone areas of Sri Lanka during a dry season. The basic parameters such as relative water supply (RWS), vegetation indices, water productivity (*WP*), ET_p and ET_a (potential and actual *ET*) were already standard products that were used widely in the monitoring irrigation performance by remote sensing [13]. The result showed that remote sensing measurements could help objectively analyze irrigation processes throughout the country and at a monthly time step.

The Yellow River is the main source of water in the delta for irrigation, industry, residential use, and livestock. This paper discussed *ET* estimation (potential and actual *ET*) according to the SEBAL algorithm in the Yellow River Delta (YRD) in China and the further potential irrigation demand to confirm the accuracy of this method application on better management of water policy-making in this area.

2. Materials and methods

2.1. The research area

The YRD is situated between 118°–119°20′E, and 36°50′–38°10′N in Shandong Province of China, facing Bohai Bay in the north, Laizhou Bay and Weifang municipality in the east, Binzhou district in the west, and Zibo municipality in the south. The irrigable farmland and the location of the study area in China are shown in Fig. 1. Historically the total area of the YRD has increased with time, as the Yellow River created by sedimentation 1000–3000 ha of new land per year in the sea at its mouth. However, in recent years the YRD has experienced land loss to the sea because of reduced sediment loads from the Yellow River resulting from heavy upstream water use. There are six agricultural irrigation regions and about 220,000 ha of arable land in the YRD, the arable fields cover 40% of the area, and are the dominant land use. With the development of the economy in northern China and the increase of population, there is a great shortage of water, and more than half of the arable land needs to be irrigated. So irrigation is the largest consumer of fresh water in this region. The area has a monsoon climate of a warm-temperate zone. Four seasons can be distinguished: a dry cold winter, a dry warm spring, a humid hot summer, and a temperate autumn. The average total sunshine is 2190–2380 hours per year.

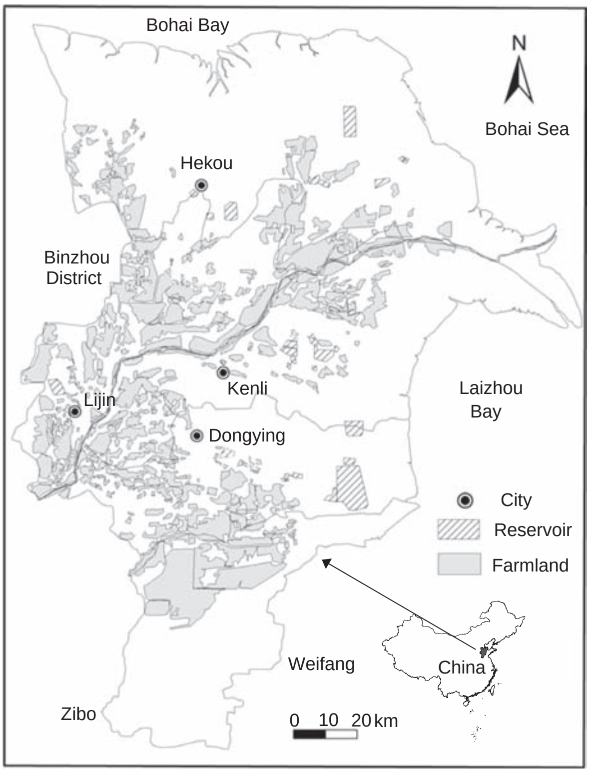

Fig. 1. Location of the study area in China.

The average annual temperature is 11.7–12.6°C. The frost-free period lasts 211 days. The average annual precipitation is 530–630 mm, of which 70% is rainfall during the summer. Average annual potential *ET* is 1900–2400 mm pan evaporation)

2.2. Source of data

The U.S. National Oceanic and Atmospheric Administration Avanced Very High Resolution Radiometer (NOAA-AVHRR) daily 1.1 km data were retrieved from the NOAA Satellite Achieve (SAA) using the following Internet site: www.saa.noaa.gov and Landsat Thematic Mapping images were ordered from the China Remote Sensing Satellite Ground Station. These images were used to compute the land surface parameters for accumulated actual ET and accumulated potential ET of the six agricultural irrigation regions. Rainfall data, wind speed, and air temperature for the YRD were obtained from the local weather stations (Kenli, Lijin and Hekou station, see Fig. 1). The irrigation supply was obtained from the Yellow River Water Resources Gazette.

2.3. The SEBAL algorithm

In the SEBAL model, *ET* is estimated as the residual of an energy balance applied to the land surface for each pixel of a satellite image:

$$\lambda E = R_n - G_0 - H \tag{1}$$

where λE is the latent heat flux (Wm^{-2}) which is readily converted to *ET* (mm), R_n is the net amount of radiation received by the surface (W·m^{-2}), H is the sensible heat flux (W·m^{-2}), and G_0 is soil heat flux (W·m^{-2}). In equation 1, net radiation is computed from the land surface radiation balance as:

$$R_n = (1-\alpha)\times R_{swd} + \varepsilon L_{in} - L_{out} \tag{2}$$

where α is the surface albedo, R_{swd} is the solar radiation (W·m^{-2}), ε is the land surface emissivity, L_{in} and L_{out} are the incoming and emitted outgoing long wave radiation (W·m^{-2}). α is determined by integrating the spectral reflectance of the satellite images, and L_{in} and L_{out} are computed as a function of surface temperature derived from the satellite images. ε is computed from vegetation indices derived from two of the short-wave bands.

Soil heat flux G_0 is empirically estimated using a function developed by Bastiaanssen (2000) [5–6] based on albedo, surface temperature (T_s in K), and normalized difference vegetation index (NDVI):

$$G_0 = \left[\frac{T_s - 273.16}{\alpha}(0.0038\alpha + 0.0074\alpha^2)(1-0.98NDVI^4)\right]R_n \tag{3}$$

Sensible heat flux H is estimated from wind speed and surface temperature using a unique "internal calibration" of the near surface to air temperature difference (*dT*) as described by Bastiaanssen (1998) [4] and Bastiaanssen and Chandrapala (2003) [14]:

$$H = \frac{\rho_a C_p (a + b\times T_s)}{r_{ah}} \tag{4}$$

where ρ_a is the air density (kg·m^{-3}) which is a function of not only atmospheric pressure, but also temperature. C_p is the specific heat capacity of air (≈1,004 J·kg^{-1}·K^{-1}), and r_{ah} is the aerodynamic resistance to heat transport (s·m^{-1}), and "*a*" and "*b*" are empirical coefficients calibrated for each image. The definition of coefficients "*a*" and "*b*" requires the selection of two extreme pixels within the scene (called cold and hot pixels), where the *dT* values can be back calculated using a known *H* at the two pixels. In the SEBAL model, the operator assigns the T_s from a water surface pixel as the "cold pixel" of SEBAL. A hot, dry (typically bare soil surface) pixel is selected as the "hot pixel" of SEBAL. Sensible heat is assumed to be zero for the cold pixel, where $\lambda E = R_n - G_0$, and $H = R_n - G_0$ for the hot pixel. The coefficients "*a*" and "*b*" in equation 4 are calibrated for each image using a linear interpolation based on T_s between these two extreme pixels.

In equation 4, r_{ah} is calculated as:

$$r_{ah} = \frac{1}{ku^*}\left[\ln\left(\frac{z-d}{z_{0h}}\right) - \Psi_h\left(\frac{z-d}{L}\right) + \Psi_h\left(\frac{z_{0h}}{L}\right)\right] \tag{5}$$

where u^* is the friction velocity, k is von Karman's constant (0.41), z is the height above the ground surface, d is the zero plane displacement height, Z_{0h} is the scalar roughness height for heat transfer, Ψ_h is the stability correction function for sensible heat transfer, and L is the Obukhov length defined as:

$$L = -\rho_a C_p u^{*3}\theta_v / kgH \tag{6}$$

where g is the acceleration due to gravity, and θ_v is the potential virtual temperature near the surface.

Once the latent heat flux at the image acquisition time is estimated by Eq. (1), an Evaporative Fraction (Λ) is calculated for the instantaneous values in the image as:

$$\Lambda = \frac{\lambda E}{R_n - G_0} \tag{7}$$

where the values for R_n, G_0, and H are instantaneous values taken from processed images. Units for all flux parameters are expressed as W·m^{-2}.

When the evaporative fraction is known, the daily actual evaporation is calculated by the following equation (SEBAL assumes that the value for Λ is constant throughout the day):

$$ET_{24} = \frac{86400\Lambda(R_{n24} - G_{024})}{\lambda\rho_w} \tag{8}$$

where R_{n24} is the daily net radiation; G_{024} is the daily soil heat flux; 86,400 is the number of seconds in a 24 h period; λ is the latent heat of vaporization (J·kg^{-1}); and ρ_w is the density of water (kg·m^{-3}). The latent heat of vaporization allows expression of ET_{24} in mm·d^{-1}.

In equation 8, G_{024} can be approximated for vegetative and soil surfaces as zero at the soil surface.

The equation for calculating R_{n24} under conditions of clear sky (all day) is:

$$R_{n24} = (1-\alpha)K_{24}^{\downarrow} + L_{24} \tag{9}$$

where $K_{24}^{\downarrow}$ is the daily incoming global radiation, and L_{24} is the daily net long wave radiation. A cumulative ET map can be derived from the daily ET maps made with a set of weather data, using linear interpolation between useable image days.

2.4. Estimation of potential ET and performance indicators

Daily estimation of potential ET (ET_p) can be calculated for irrigation scheduling from the Priestly and Taylor (1972) method [15], which is a simple form of the Penman-Monteith equation, using the satellite data [16]:

$$ET_p = 1.26 \times R_{n24}\left(\frac{\Delta}{\Delta+\gamma}\right) \tag{10}$$

where ET_p is potential ET (W·m^{-2}), Δ is slope of the water saturation vapor pressure curve (mbar·K^{-1}), and γ is the psychrometric constant (mbar·K^{-1}).

Increasing food production with limited water resources is the main challenge for irrigated agriculture in the 21st Century; therefore, monitoring the performance of irrigated systems is meaningful. The term "performance" of an irrigation system can be quantified by factors such as water inflow, crop demand, water use, system losses, crop production, and the extent cultivated [12]. No standard method is available to make a performance assessment for an irrigation system. Irrigation performance indicators are mainly concerned with the assessment of the water flow path in a given irrigation system. The objective of irrigation managers is to minimize water deficit to a crop during its growing stages. The ET deficit is very important for irrigation management. The ET deficit (ET_d) is the difference between ET_p and actual ET_a in absolute terms, which can be calculated as:

$$ET_d = ET_p - ET_a\ (\text{mm}\cdot\text{d}^{-1}) \tag{11}$$

Water depletion is a key concept of water accounting, but in irrigation practice, irrigation efficiency is more important for the system managers. Irrigation efficiency was defined by Bos and Nugteren (1974) [17] as the irrigation demand (crop ET minus effective rainfall) divided by irrigation supply, assuming that crop ET is at the potential level. It is very difficult to compute the contribution from effective rainfall to the actual ET.

Relative water supply (*RWS*) as presented by Levine (1982) [18] is the ratio of total water supply to the total crop demand. At the irrigation system level, the total water supply is the total amount of water flowing into the domain from precipitation plus any irrigation supply from diversion and groundwater pumping. Crop demand is potential evapotranspiration under well-watered conditions. Hence, for the YRD, *RWS* can be expressed as:

$$RWS = \frac{P + IS}{ET_p} \tag{12}$$

Where P is precipitation, and IS is irrigation supply. It should be noted that, this ratio (*RWS*) does not reflect whether the crop has received the correct amount of water at the correct time but emphasizes the overall situation of water supply and demand. The ratio does not indicate how effectively the water supply has been utilized.

The water performance indicator used in this study is the ET deficit and RWS and WRn (net crop water requirement). So in the present work, the first task is to calculate the actual ET, potential ET and volume of the crop water requirements, which can be calculated using the SEBAL model.

3. Results and discussion

3.1. Actual ET

Applying the SEBAL model to the Landsat image of the YRD Irrigation District, captured on 2 May 2000, the daily actual ET (ET_a) map was produced (Fig. 2). The light gray tones located in the irrigable land represent high ET_a (irrigated area and water body), which varied between 3 and 5.6 mm·d^{-1}, and the darker tones represented low ET_a (natural vegetation and bare soil). The limits of the irrigable area were delineated on Fig. 1. Seen from the ET_a map, these irrigable areas from Lijin to Kenli near the Yellow River have higher ET_a, and this indicated that these irrigation regions got more water than other places.

The yearly and seasonal ET_a were obtained from the NOAA-AVHRR images by applying the SEBAL algorithm. The yearly actual ET varied between 710 and 910 mm for the irrigated land in 2000 (Fig. 2), and between 600 and 920 mm for the whole area, including bare ground and water body. The average daily ET_a for the local mixture of agricultural crops was

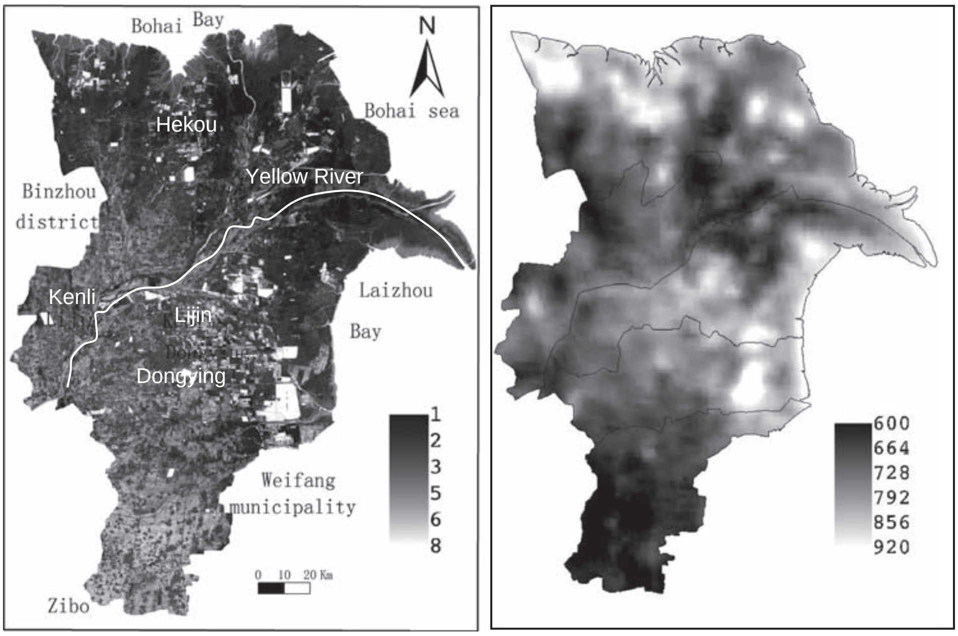

Fig. 2. Daily actual *ET* map (left) and yearly *ET* map (right) for the Yellow River Delta (mm).

$840/365 = 2.3$ mm·d^{-1}. In the YRD the main crops are winter wheat and cotton. The ET_a for cotton from April to October varied between 522 and 731 mm with an average of 621 mm, and for winter wheat from October 2000 to May 2001 the ET_a varied between 360 and 620 mm with an average of 497 mm.

Higher ET_a in the irrigated area also occurred in the districts of Lijin, Kenli and Dongying near the Yellow River, and this indicated that these areas had a better-irrigated condition than other places. In fact, these areas are near the Yellow River and easily obtain water supply from the river.

In the YRD, the arable land is 228,917 ha, the irrigable area is 144,170 ha, the irrigated area is 128,570 ha, and the water delivery from the Yellow River in 2000 was 6.22×10^8 m^3 (483.8 mm for irrigated land). The precipitation was 319.6 mm for the cropping season, and the local runoff in the YRD was 32 mm in 2000. The groundwater table was mildly decreasing according to field information. The mildly decreasing water table behavior revealed that irrigation water plus effective rainfall may be smaller than ET_a for the irrigated areas. In fact, ET_a for the irrigated areas in 2000 slightly exceeded the irrigation water plus effective rainfall 19.6 mm ($791 - 6220/12.8570 - 319.6 + 32 = 19.6$), and this indicated that the estimation results were reasonable for meeting the actual situation. Figure 3 showed the monthly distribution of ET_a and precipitation for the Lijin irrigation system in 2000, and it revealed that ET_a was much more than the precipitation in most months, with the exception of July. So in the YRD, most months need irrigation water supply for farmland.

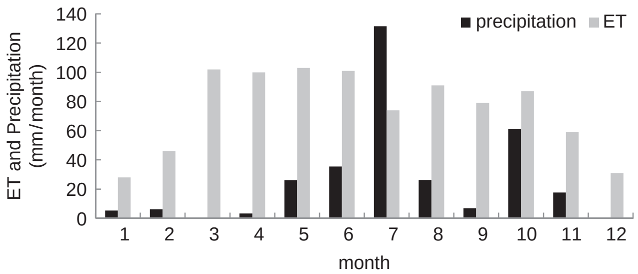

Fig. 3. Monthly estimated actual *ET* and precipitation for the Lijin irrigation system in the Yellow River Delta in 2000.

3.2. Application in water management

In order to monitor the water use and understand the irrigation efficiency, estimating the potential *ET* is very important. The potential ET, estimated by the Priestley and Taylor (1972) [15] method using remotely sensed data, was 1210 mm for irrigated land, and the ET deficit was 370 mm in 2000. A higher *ET* deficit occurred in the Hekou irrigation district far from the Yellow River, and lower *ET* deficits occurred in the areas situated in the Dongying and Lijin irrigation districts near the Yellow River. The lower *ET* deficit revealed that these regions were well irrigated, and the higher ET deficit meaned

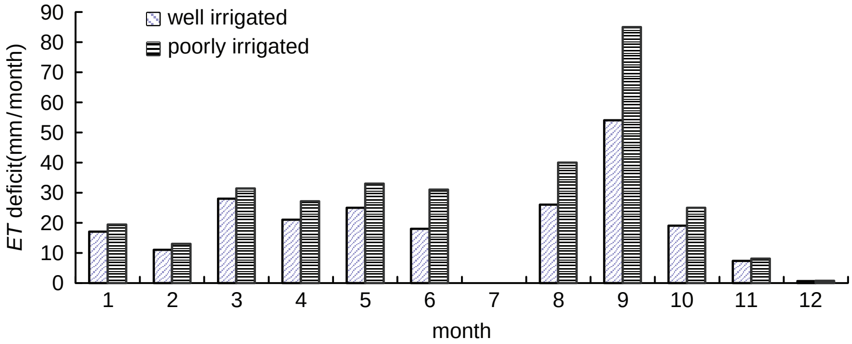

Fig. 4. Monthly estimated *ET* deficit for better and poorly irrigated areas in the Yellow River Delta in 2000.

these areas were poorly irrigated. Figure 4 showed the monthly *ET* deficit under the different irrigation conditions in 2000. Seen from the Fig. 4, the *ET* deficit in July and December equaled zero showing that the water supply satisfied the crop demand, and in the other months the *ET* deficit was bigger, especially in September, the water supply do did not satisfy the crop water requirements.

The spatial variation in the ET deficit of the YRD irrigation district also indicated the spatial variation in crop growth and the relative soil wetness. Each month's ET deficit indicated the crop growth, and the ET deficit map of each month revealed that the crops in the Lijin and Dongying irrigation districts grew in a better water resource condition in 2000.

The relative water supply was computed according to equation (12) for the total irrigated land in the YRD. The RWS related the water made available for crops, including surface irrigation, groundwater pumped and rainfall, to the amount crops need. This indicator provided information about the relative abundance or scarcity of water. Seen from the results, the RWS varied between 48 and 91% with an average of 70%, and the higher RWS was distributed along the Yellow River. This implied that the irrigation water volume did not exceed the crop water demand and the area along the Yellow River was relative abundance of water.

Irrigation demand was also important for water resources management. It can be estimated by: ET_p minus effective precipitation. The winter wheat ET_p was 667 mm during October 2000 to May 2001, and the cotton ET_p was 814 mm from April to October in 2000. So the irrigation demand for winter wheat was $667 - 135 = 532$ mm, and $814 - 207 = 607$ mm for cotton.

The net crop water requirements (*WRn*) for the irrigated land are also estimated by subtracting the effective precipitation from ET_a. The *WRn* varied between 154 and 415 mm in the YRD in 2000–2001 for winter wheat with an average *WRn* of 290 mm. The *WRn* varied between 316 and 525 mm for cotton in 2000 with an average of 415 mm. The volume of net water requirements was also obtained for the YRD area jointly with the digital crop maps and *WRn* values. For winter wheat, the irrigated area was 67,991 ha, and the volume of net water requirements was $67{,}991 \times 0.290 \times 10^4$m, that was 1.97×10^8 m^3. The irrigated area for cotton was 39,186 ha, and the volume of net water requirements was $39{,}186 \times 0.415 \times 10^4$ m^3, that was 1.63×10^8 m^3.

4. Conclusions

Applying the SEBAL model estimates of the ET_a and ET_p can be obtained with higher accuracy in the YRD. Time series of ET_a are now emerging as important combined temporal and spatial analysis tools for water consumption by irrigated crops. Assessment of the performance of irrigated crops revealed that water delivery did not exceed the crop requirements, and the *WRn* for cotton and wheat were smaller than the irrigation demand. The method results can provide truly spatial information to help decision-makers to improve current water policies in the YRD.

Acknowledgement

This work is supported by National Natural Science Foundation project (40871219) and (40971258). The authors are most grateful to Dr. Charles S. Melching from Marquette University, USA and two anonymous reviewers for detailed review and valuable comments, which contributed to an improvement of the manuscript.

References

[1] J. Zwart Sander and W.G.M. Bastiaanssen SEBAL for detecting spatial variation of water productivity and scope for improvement in eight irrigated wheat systems. Agricultural Water Management, 89 (2007) 287–296.

[2] W.P. Kustas and J.M. Norman. Use of remote sensing for evapotranspiration monitoring over land surfaces. Hydrological Sciences—Journal—des Sciences Hydrologiques, 41(1996) 495–516.
[3] W.G.M. Bastiaanssen. Regionalization of surface flux densities and moisture indicators in composite terrain. In: a remote sensing approach under clear skies in Mediterranean climates. Agricultural Research Department, Report 109, Wageningen, the Netherlands 1995.
[4] W.G.M. Bastiaanssen. Remote sensing in water resources management: the state of the art. International Irrigation Management Institute. Colombo, Sri Lanka 1998, p. 118.
[5] W.G.M. Bastiaanssen. SEBAL-based sensible and latent heat fluxes in the irrigated Gediz Basin, Turkey. J. Hydrol., 229 (2000) 87–100.
[6] W.G.M. Bastiaanssen, David J. Molden and Ian W. Makin. Remote sensing for irrigated agriculture: examples from research and possible applications. Agricultural Water Management, 46 (2000) 137–155.
[7] Z.A. Su. Surface Energy Balance System (SEBS) for estimation of turbulent heat fluxes from point to continental scale. Publications of the National Remote Sensing Board (BCRS), USP-2, 01-02 (2001) 183.
[8] B.J. Choudhury, N.U. Ahmed, S.B. Idso and R.J. Reginato, C.S.T. Daughtry. Relations between evaporation coefficients and vegetation indices studied by model simulations. Rem. Sens. Environ. 50 (1994) 1–17.
[9] A. Rango and A. Shalaby. Operational applications of remote sensing in hydrology success prospects and problems. IAHS Hydrol. Sci. J., 43 (1998) 947–968.
[10] W.G.M. Bastiaanssen and M.G. Bos Irrigation performance indicators based on remotely sensed data: a review of literature. Irrigation and Drainage Systems, 13 (1999) 291–311.
[11] J.B. Stewart, C.J. Watts, J.C. Rodriguez, H.A.R. de Bruin, A.R. van de Berg and J. Garatuza-Payan. Use of satellite data to estimate radiation and evaporation for northwest Mexico. Agricultural water management, 38 (1999) 181–193.
[12] K.M.P.S. Bandara. Monitoring irrigation performance in Sri Lanka with high-frequency satellite measurements during the dry season. Agricultural Water Management, 58 (2003) 159–170.
[13] M. Akbari, N. Toomanian, P. Droogers, W. Bastiaanssen, and A. Gieske. Monitoring irrigation performance in Esfahan, Iran, using NOAA satellite imagery. Agricultural Water Management, 88 (2007) 99–109.
[14] W.G.M. Bastiaanssen and L. Chandrapala. Water balance variability across Sri Lanka for agricultural environmental water use. Agricultural Water Management, 58 (2003) 171–192.
[15] C.H.B. Priestley and R.J. Taylor. On the assessment of the surface heat flux and evapotranspiration using large scale parameters. Monthly Weath. Rev., 100 (1972) 81–92.
[16] M.G. Mekonnen, W.G.M. Bastiaanssen. A new simple method to determine crop-water requirements from satellite data: results from Kenya. Irrig. Drainage Syst., 14 (2000) 237–256.
[17] M.G. Bos, J. Nugteren. On irrigation efficiencies. ILRI Publications No. 19. International Institute for Land Reclamation and Improvement (ILRI), Wageningen, The Netherlands, 1974.
[18] G. Levine. Relative water supply: an explanatory variable for irrigation system. Technical Report, No.6, Cornell University, Ithaca, NY, USA 1982.